Physics Letters B 840 (2023) 137835

Contents lists available at ScienceDirect

Physics Letters B

journal homepage: www.elsevier.com/locate/physletb

Corrigendum

Corrigendum: "Measurement of ^{73}Ge(n, γ) cross sections and implications for stellar nucleosynthesis" [Phys. Lett. B 790 (2019) 458–465]

C. Lederer-Woods[a,b,*], U. Battino[a], P. Ferreira[c], A. Gawlik[d], C. Guerrero[e], F. Gunsing[f,g], S. Heinitz[h], J. Lerendegui-Marco[e], A. Mengoni[i], R. Reifarth[b], A. Tattersall[a], S. Valenta[j], C. Weiss[g,m], O. Aberle[g], J. Andrzejewski[d], L. Audouin[k], V. Bécares[l], M. Bacak[m], J. Balibrea[l], M. Barbagallo[n], S. Barros[c], F. Bečvář[j], C. Beinrucker[b], F. Belloni[f], E. Berthoumieux[f], J. Billowes[o], D. Bosnar[p], M. Brugger[g], M. Caamaño[q], F. Calviño[r], M. Calviani[g], D. Cano-Ott[l], F. Cerutti[g], E. Chiaveri[g], N. Colonna[n], G. Cortés[r], M.A. Cortés-Giraldo[e], L. Cosentino[s], L.A. Damone[n,t], K. Deo[u], M. Diakaki[f,v], M. Dietz[a], C. Domingo-Pardo[w], R. Dressler[h], E. Dupont[f], I. Durán[q], B. Fernández-Domínguez[q], A. Ferrari[g], P. Finocchiaro[s], R.J.W. Frost[o], V. Furman[x], K. Göbel[b], A.R. García[l], I. Gheorghe[y], T. Glodariu[y], I.F. Gonçalves[c], E. González-Romero[l], A. Goverdovski[z], E. Griesmayer[m], H. Harada[aa], T. Heftrich[b], A. Hernández-Prieto[g,r], J. Heyse[ab], D.G. Jenkins[ac], E. Jericha[m], F. Käppeler[ad], Y. Kadi[g], T. Katabuchi[ae], P. Kavrigin[m], V. Ketlerov[z], V. Khryachkov[z], A. Kimura[aa], N. Kivel[h], I. Knapova[j], M. Kokkoris[v], M. Krtička[j], E. Leal-Cidoncha[q], H. Leeb[m], M. Licata[af,ag], S. Lo Meo[i,af], R. Losito[g], D. Macina[g], J. Marganiec[d], T. Martínez[l], C. Massimi[af,ag], P. Mastinu[ah], M. Mastromarco[n], F. Matteucci[ai,aj], E. Mendoza[l], P.M. Milazzo[ai], F. Mingrone[af], M. Mirea[y], S. Montesano[g], A. Musumarra[s,ak], R. Nolte[al], F.R. Palomo-Pinto[e], C. Paradela[q], N. Patronis[am], A. Pavlik[an], J. Perkowski[d], J.I. Porras[g,ao], J. Praena[e], J.M. Quesada[e], T. Rauscher[ap,aq], A. Riego-Perez[r], M. Robles[q], C. Rubbia[g], J.A. Ryan[o], M. Sabaté-Gilarte[g,e], A. Saxena[u], P. Schillebeeckx[ab], S. Schmidt[b], D. Schumann[h], P. Sedyshev[x], A.G. Smith[o], A. Stamatopoulos[v], S.V. Suryanarayana[u], G. Tagliente[n], J.L. Tain[w], A. Tarifeño-Saldivia[w], L. Tassan-Got[k], A. Tsinganis[v], G. Vannini[af,ag], V. Variale[n], P. Vaz[c], A. Ventura[af], V. Vlachoudis[g], R. Vlastou[v], A. Wallner[ar], S. Warren[o], M. Weigand[b], T. Wright[o], P. Žugec[p]

[a] School of Physics and Astronomy, University of Edinburgh, United Kingdom
[b] Goethe University Frankfurt, Germany
[c] Instituto Superior Técnico, Lisbon, Portugal
[d] University of Lodz, Poland
[e] Universidad de Sevilla, Spain
[f] CEA Irfu, Université Paris-Saclay, F-91191 Gif-sur-Yvette, France
[g] European Organization for Nuclear Research (CERN), Switzerland
[h] Paul Scherrer Institut (PSI), Villingen, Switzerland
[i] Agenzia nazionale per le nuove tecnologie, l'energia e lo sviluppo economico sostenibile (ENEA), Bologna, Italy
[j] Charles University, Prague, Czech Republic
[k] Institut de Physique Nucléaire, CNRS-IN2P3, Univ. Paris-Sud, Université Paris-Saclay, F-91406 Orsay Cedex, France
[l] Centro de Investigaciones Energéticas Medioambientales y Tecnológicas (CIEMAT), Spain
[m] Technische Universität Wien, Austria
[n] Istituto Nazionale di Fisica Nucleare, Sezione di Bari, Italy
[o] University of Manchester, United Kingdom

DOI of original article: https://doi.org/10.1016/j.physletb.2019.01.045.
* Corresponding author at: School of Physics and Astronomy, University of Edinburgh, United Kingdom.
E-mail address: claudia.lederer-woods@ed.ac.uk (C. Lederer-Woods).

https://doi.org/10.1016/j.physletb.2023.137835

[p] Department of Physics, Faculty of Science, University of Zagreb, Zagreb, Croatia
[q] University of Santiago de Compostela, Spain
[r] Universitat Politècnica de Catalunya, Spain
[s] INFN Laboratori Nazionali del Sud, Catania, Italy
[t] Dipartimento di Fisica, Università degli Studi di Bari, Italy
[u] Bhabha Atomic Research Centre (BARC), India
[v] National Technical University of Athens, Greece
[w] Instituto de Física Corpuscular, CSIC - Universidad de Valencia, Spain
[x] Joint Institute for Nuclear Research (JINR), Dubna, Russia
[y] Horia Hulubei National Institute of Physics and Nuclear Engineering, Romania
[z] Institute of Physics and Power Engineering (IPPE), Obninsk, Russia
[aa] Japan Atomic Energy Agency (JAEA), Tokai-mura, Japan
[ab] European Commission, Joint Research Centre, Geel, Retieseweg 111, B-2440 Geel, Belgium
[ac] University of York, United Kingdom
[ad] Karlsruhe Institute of Technology, Campus North, IKP, 76021 Karlsruhe, Germany
[ae] Tokyo Institute of Technology, Japan
[af] Istituto Nazionale di Fisica Nucleare, Sezione di Bologna, Italy
[ag] Dipartimento di Fisica e Astronomia, Università di Bologna, Italy
[ah] Istituto Nazionale di Fisica Nucleare, Sezione di Legnaro, Italy
[ai] Istituto Nazionale di Fisica Nucleare, Sezione di Trieste, Italy
[aj] Dipartimento di Astronomia, Università di Trieste, Italy
[ak] Dipartimento di Fisica e Astronomia, Università di Catania, Italy
[al] Physikalisch-Technische Bundesanstalt (PTB), Bundesallee 100, 38116 Braunschweig, Germany
[am] University of Ioannina, Greece
[an] University of Vienna, Faculty of Physics, Vienna, Austria
[ao] University of Granada, Spain
[ap] Centre for Astrophysics Research, University of Hertfordshire, United Kingdom
[aq] Department of Physics, University of Basel, Switzerland
[ar] Australian National University, Canberra, Australia

ARTICLE INFO

Article history:
Received 13 February 2023
Accepted 6 March 2023
Available online 14 March 2023
Editor: D.F. Geesaman

The neutron fluence spectrum used in the analysis to determine absolute cross section values was found to be erroneous. The same error also affects data in [1], and a separate correction will be published for that work. The corrected Maxwellian averaged cross sections (MACS) are listed in Table 1 and shown in Fig. 1. The corrected resonance capture kernels and unresolved cross sections are shown in Tables 3–7, and Fig. 2, respectively. The average resonance parameters determined from the resonance fits change slightly (within uncertainties). We obtain an average radiative width of $\langle\Gamma_\gamma\rangle = 243(10)$ meV and $\sigma_{\Gamma_\gamma} = 30(5)$ meV, an average s-wave spacing of $D_0 = 74(8)$ eV, and neutron strength functions of $S_0 = 2.1(3) \times 10^{-4}$ and $S_1 = 1.5(5) \times 10^{-4}$. Uncertainties in the resonance kernels due to systematic effects are 3.9% below and 6.0% above 10 keV neutron energy, consisting of uncertainties due to Pulse Height Weighting (3%), normalisa-

Table 1
Ground state Maxwellian averaged cross sections on ^{73}Ge, and stellar Maxwellian averaged cross sections, taking into account neutron capture on thermally populated excited states.

kT (keV)	MACS (mb)	MACS* (mb)
5	1181 ± 48	1185 ± 59
10	722 ± 34	728 ± 55
20	455 ± 24	455 ± 46
30	346 ± 19	339 ± 39
40	284 ± 16	273 ± 34
50	243 ± 14	231 ± 30
60	214 ± 13	201 ± 27
70	192 ± 11	179 ± 25
80	175 ± 11	162 ± 23
90	161.0 ± 9.7	148 ± 22
100	149.7 ± 9.1	137 ± 21

Table 2
Uncertainties of Maxwellian averaged ^{73}Ge cross sections.

Source	Uncertainty (%)
Neutron Flux Shape	$2-5$
Weighting Functions	3
Normalisation to Au	1
Background Subtraction (> 14 keV)	1
Sample Enrichment	1
Multiple Scattering and Self Shielding (> 14 keV)	1.2
Statistics	0.3
Total	4.1-6.1

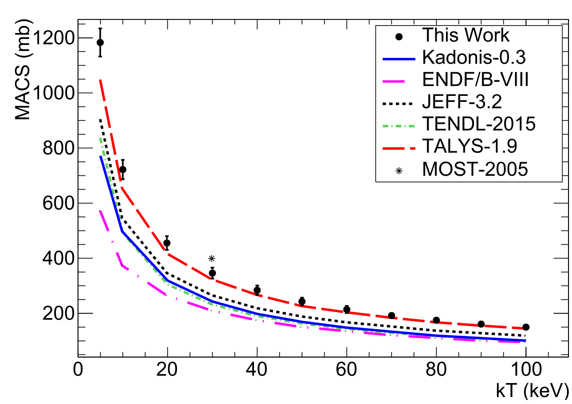

Fig. 1. Comparison of the experimental MACS from $kT = 5 - 100$ keV with evaluations and theoretical predictions [2–8]. MOST-2005 [3] and TALYS-1.9 [4] most closely reproduce the experimental values, while all others significantly underestimate the MACS by a factor of up to 2.

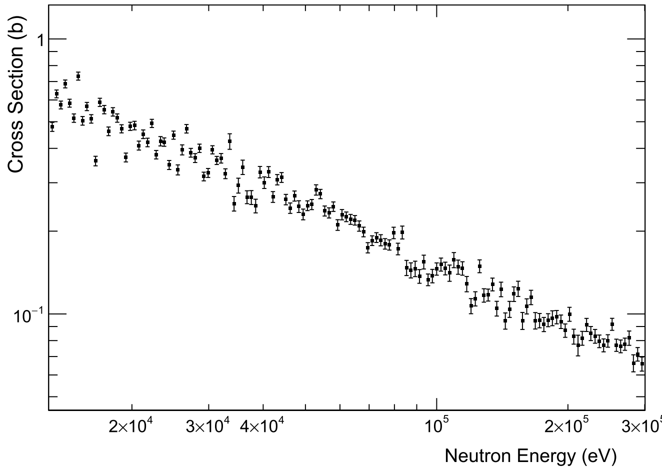

Fig. 2. Averaged cross sections from 14 keV to 300 keV neutron energy and statistical uncertainties.

Table 3
Resonance energies and capture kernels k of ^{73}Ge(n,γ) ^{a}Resonances fitted with natural germanium sample. *Resonances listed in ENDF/B-VIII [2]. ^{b}Doublet in ENDF/B-VIII [2].

E_R (eV)	K (meV)	E_R (eV)	K (meV)
59.37 ± 0.06	0.0027 ± 0.0005	$1219.96 \pm 0.02^{*}$	112.59 ± 0.89
79.47 ± 0.01	0.054 ± 0.002	1233.08 ± 0.06	11.05 ± 0.53
$102.73 \pm 0.01^{a,*}$	104.04 ± 0.63	1276.90 ± 0.05	3.86 ± 0.13
156.32 ± 0.02	0.064 ± 0.003	$1316.75 \pm 0.02^{*}$	108.65 ± 0.84
$204.15 \pm 0.01^{a,*}$	60.80 ± 0.51	$1358.03 \pm 0.02^{*}$	70.90 ± 0.71
$224.81 \pm 0.00^{*}$	74.29 ± 0.18	1380.22 ± 0.18	0.91 ± 0.09
270.90 ± 0.06	0.073 ± 0.006	1384.69 ± 0.09	1.87 ± 0.11
286.68 ± 0.02	0.204 ± 0.007	1404.78 ± 0.09	1.47 ± 0.09
$320.69 \pm 0.01^{a,*}$	63.83 ± 1.12	1462.39 ± 0.08	3.14 ± 0.15
$332.87 \pm 0.02^{a,*}$	97.14 ± 1.59	$1530.64 \pm 0.03^{*}$	119.8 ± 1.0
361.81 ± 0.06	0.47 ± 0.04	1540.43 ± 0.09	3.59 ± 0.22
$368.07 \pm 0.01^{*}$	95.95 ± 0.32	1549.35 ± 0.13	3.75 ± 0.31
$409.28 \pm 0.00^{*}$	59.61 ± 0.20	1552.27 ± 0.09	6.28 ± 0.37
479.57 ± 0.07	0.56 ± 0.04	1614.59 ± 0.26	0.47 ± 0.07
$491.48 \pm 0.01^{*}$	101.45 ± 0.47	$1655.93 \pm 0.05^{*}$	124.1 ± 1.3
$517.99 \pm 0.01^{*}$	11.91 ± 0.10	1665.37 ± 0.09	6.19 ± 0.37
$558.35 \pm 0.01^{*}$	74.05 ± 0.27	1675.03 ± 0.42	0.61 ± 0.12
$668.80 \pm 0.04^{*}$	0.94 ± 0.03	1716.18 ± 0.04	19.05 ± 0.38
693.58 ± 0.04	0.81 ± 0.03	1751.88 ± 0.18	0.98 ± 0.09
750.31 ± 0.08	0.31 ± 0.02	$1808.03 \pm 0.04^{*}$	111.3 ± 1.1
762.71 ± 0.02	3.40 ± 0.06	1843.00 ± 0.08	3.93 ± 0.19
777.47 ± 0.04	0.91 ± 0.03	1897.71 ± 0.18	1.15 ± 0.10
798.47 ± 0.06	0.44 ± 0.03	1930.82 ± 0.73	0.30 ± 0.09
816.68 ± 0.24	0.084 ± 0.015	$1952.76 \pm 0.05^{b,*}$	106.6 ± 1.2
826.23 ± 0.02	5.04 ± 0.09	1963.42 ± 0.15	3.20 ± 0.27
843.31 ± 0.03	2.95 ± 0.09	$2019.34 \pm 0.05^{*}$	118.6 ± 1.5
$851.38 \pm 0.01^{*}$	57.97 ± 0.45	2104.01 ± 0.11	3.43 ± 0.20
878.76 ± 0.08	0.73 ± 0.05	2116.60 ± 0.13	3.64 ± 0.21
$920.47 \pm 0.01^{*}$	48.99 ± 0.46	2144.12 ± 0.17	2.38 ± 0.18
948.06 ± 0.13	0.34 ± 0.04	2162.03 ± 0.03	51.86 ± 0.95
959.19 ± 0.05	1.72 ± 0.07	2211.39 ± 0.58	0.49 ± 0.11
$1031.14 \pm 0.01^{*}$	56.42 ± 0.65	2216.97 ± 0.51	0.53 ± 0.10
1059.02 ± 0.01	75.26 ± 0.64	2236.71 ± 0.41	1.03 ± 0.17
1139.18 ± 0.13	1.82 ± 0.15	$2262.52 \pm 0.05^{*}$	109.3 ± 1.6
$1148.41 \pm 0.03^{*}$	119.64 ± 0.86	2291.07 ± 0.13	118.1 ± 4.1

tion (1%), sample enrichment (1%), and neutron flux (2% below, 5% above 10 keV). Total systematic uncertainties for the averaged cross sections are 6.2% and uncertainties for the Maxwellian averaged capture cross sections change correspondingly (see Table 2). Due to the small changes of at most 4% in the Maxwellian averaged capture cross section (smaller than the total uncertainty), all conclusions remain unaltered. The authors apologise for any inconvenience this caused. Updated data will be provided to the EXFOR database.

Table 4
Table 3 continued.

E_R (eV)	K (meV)	E_R (eV)	K (meV)
$2297.88 \pm 0.07^{*}$	104.7 ± 3.9	3431.09 ± 0.66	6.8 ± 2.5
2321.90 ± 0.07	16.70 ± 0.57	3432.30 ± 0.59	7.2 ± 2.5
2373.27 ± 0.12	6.58 ± 0.34	3495.69 ± 0.54	1.59 ± 0.26
2398.90 ± 0.29	1.47 ± 0.19	3535.63 ± 0.08	38.8 ± 1.1
2442.65 ± 0.04	106.7 ± 1.5	3565.09 ± 0.35	3.87 ± 0.42
2531.55 ± 0.23	2.33 ± 0.22	3579.46 ± 0.08	34.7 ± 1.1
$2566.67 \pm 0.06^{*}$	118.0 ± 1.6	3628.37 ± 0.32	3.49 ± 0.36
2624.55 ± 0.13	6.96 ± 0.43	3657.50 ± 0.16	17.67 ± 0.87
$2648.06 \pm 0.06^{*}$	26.81 ± 0.69	3674.49 ± 0.06	92.5 ± 2.0
2666.79 ± 0.05	54.1 ± 1.3	3718.10 ± 0.07	71.0 ± 1.8
2688.08 ± 0.05	107.2 ± 1.8	3745.17 ± 0.19	9.00 ± 0.54
2697.88 ± 0.13	8.48 ± 0.53	3763.27 ± 0.25	4.74 ± 0.40
$2748.80 \pm 0.39^{*}$	2.14 ± 0.29	3809.15 ± 0.59	4.15 ± 0.97
2763.66 ± 0.28	2.79 ± 0.31	3812.80 ± 0.46	3.94 ± 0.85
2776.01 ± 0.05	48.9 ± 1.0	3852.86 ± 0.15	21.10 ± 0.93
2806.78 ± 0.18	3.91 ± 0.30	3870.01 ± 0.09	48.3 ± 1.4
2821.47 ± 0.35	2.05 ± 0.22	3993.95 ± 0.30	7.63 ± 0.67
2903.85 ± 0.17	5.19 ± 0.35	4002.59 ± 0.44	3.79 ± 0.46
2924.79 ± 0.14	11.86 ± 0.63	4042.61 ± 0.26	19.1 ± 1.8
2946.15 ± 0.08	113.0 ± 1.9	4053.75 ± 0.25	143.5 ± 3.9
2982.64 ± 0.05	52.9 ± 1.2	4073.85 ± 0.08	86.7 ± 3.0
$3005.30 \pm 0.86^{*}$	1.02 ± 0.29	4215.87 ± 0.20	16.47 ± 0.91
3023.48 ± 0.05	102.0 ± 1.9	4246.62 ± 0.25	107.1 ± 4.1
3037.63 ± 0.08	36.8 ± 1.2	4254.80 ± 0.12	68.2 ± 3.6
3044.65 ± 0.61	1.87 ± 0.40	$4349.24 \pm 0.10^{*}$	60.3 ± 1.7
3085.74 ± 0.36	2.25 ± 0.27	4394.73 ± 0.21	16.2 ± 1.0
3133.34 ± 0.56	1.66 ± 0.29	4406.67 ± 0.14	34.8 ± 1.6
3155.23 ± 0.06	90.3 ± 1.6	$4419.24 \pm 0.56^{*}$	3.80 ± 0.58
3214.08 ± 0.14	8.93 ± 0.52	4458.64 ± 0.13	134.6 ± 3.0
3251.24 ± 0.07	29.21 ± 0.84	4475.90 ± 0.29	15.2 ± 1.2
3264.48 ± 0.43	1.17 ± 0.20	4499.19 ± 0.11	107.0 ± 2.7
3320.64 ± 0.17	8.74 ± 0.52	4548.87 ± 0.26	16.4 ± 1.2
3361.67 ± 0.10	38.2 ± 1.2	4564.62 ± 0.10	115.9 ± 2.8
3388.25 ± 0.29	5.98 ± 0.49	4635.78 ± 0.10	68.9 ± 2.0
3414.95 ± 0.07	47.6 ± 6.1	4649.66 ± 0.48	4.14 ± 0.58

Table 5
Table 3 continued.

E_R (eV)	K (meV)	E_R (eV)	K (meV)
4753.84 ± 0.46	8.4 ± 1.1	6040.11 ± 0.15	134.7 ± 4.0
4759.61 ± 0.46	7.5 ± 1.1	$6075.57 \pm 0.16^{*}$	120.9 ± 3.9
4828.05 ± 0.30	29.8 ± 2.1	6136.59 ± 0.60	9.28 ± 0.93
4837.18 ± 0.35	52.6 ± 5.8	6155.00 ± 0.60	8.6 ± 1.1
4843.11 ± 0.17	138.2 ± 6.9	6219.66 ± 0.16	149.6 ± 4.4
4898.05 ± 0.55	6.92 ± 0.81	6241.34 ± 0.16	84.9 ± 3.1
4949.77 ± 0.29	12.81 ± 0.97	6279.24 ± 0.41	23.2 ± 2.0
5039.55 ± 0.22	22.3 ± 1.2	6289.64 ± 0.39	23.3 ± 2.1
5061.31 ± 0.13	57.9 ± 2.2	6327.12 ± 0.41	27.8 ± 2.4
5098.09 ± 0.41	12.9 ± 1.2	6344.30 ± 0.19	126.8 ± 4.1
$5106.75 \pm 0.22^{*}$	23.4 ± 1.5	6400.4 ± 1.3	4.5 ± 1.3
5126.36 ± 0.44	6.22 ± 0.74	$6427.66 \pm 0.19^{*}$	57.5 ± 2.4
5160.93 ± 0.41	7.02 ± 0.71	6455.7 ± 1.8	2.95 ± 0.89
5207.89 ± 0.17	120.5 ± 3.5	6470.55 ± 0.27	38.5 ± 2.3
5220.23 ± 0.31	2.5 ± 1.2	6485.65 ± 0.38	23.4 ± 1.9
5245.99 ± 0.14	51.8 ± 1.9	6504.19 ± 0.18	59.2 ± 2.4
5281.73 ± 0.13	124.4 ± 3.2	6578.24 ± 0.25	134.3 ± 4.9
5302.89 ± 0.93	6.1 ± 1.2	6602.48 ± 0.36	97 ± 10
5312.61 ± 0.23	32.3 ± 2.1	6616.73 ± 0.62	160 ± 28
5364.06 ± 0.24	110.6 ± 4.8	6626.32 ± 0.63	113 ± 21
$5381.64 \pm 0.25^{*}$	132.4 ± 5.4	6739.99 ± 0.26	3.1 ± 1.5
5419.93 ± 0.12	130.0 ± 3.4	6766.28 ± 0.16	159.5 ± 4.9
5485.82 ± 0.25	18.3 ± 1.2	6826.23 ± 0.85	8.6 ± 1.2
5506.04 ± 0.38	9.40 ± 0.85	6866.12 ± 0.21	104.7 ± 3.9
5547.04 ± 0.45	8.34 ± 0.90	6883.41 ± 0.57	15.8 ± 2.0
$5598.25 \pm 0.14^{*}$	95.6 ± 3.1	6955.69 ± 0.19	91.1 ± 3.4
$5612.69 \pm 0.42^{*}$	8.4 ± 1.0	6974.01 ± 0.59	11.5 ± 1.5
5681.92 ± 0.37	14.9 ± 1.2	$7118.06 \pm 0.20^{*}$	81.2 ± 3.2
5716.42 ± 0.14	117.9 ± 3.2	7154.31 ± 0.08	12.3 ± 4.4
5765.08 ± 0.22	138.4 ± 4.2	7177.27 ± 0.38	41.2 ± 2.7
5815.34 ± 0.22	43.8 ± 2.4	7221.40 ± 0.18	124.4 ± 4.9
5873.41 ± 0.18	93.4 ± 3.3	7245.55 ± 0.52	24.3 ± 2.4
5927.51 ± 0.44	9.5 ± 1.6	7290.68 ± 0.27	137.3 ± 5.0
5975.45 ± 0.64	6.85 ± 0.86	7330.82 ± 0.31	137.2 ± 5.3
6002.51 ± 0.27	36.4 ± 2.0	7370.58 ± 0.24	90.5 ± 4.0

Table 6
Table 3 continued.

E_R (eV)	K (meV)	E_R (eV)	K (meV)
7480.93 ± 0.20	68.5 ± 3.0	9038.39 ± 0.25	129.3 ± 3.3
7507.9 ± 1.3	7.6 ± 1.5	9086.31 ± 0.54	46.7 ± 4.1
7601.57 ± 0.22	87.6 ± 3.4	9097.10 ± 0.93	21.6 ± 3.4
7641.77 ± 0.21	143.1 ± 4.8	9147.3 ± 1.7	15.2 ± 2.7
7756.09 ± 0.75	15.3 ± 1.8	9168.5 ± 1.3	12.1 ± 2.3
7777.38 ± 0.35	36.2 ± 2.5	9191.3 ± 1.0	26.2 ± 3.6
7830.12 ± 0.71	23.5 ± 2.5	9209.90 ± 0.97	51.5 ± 9.9
7862.18 ± 0.52	114.8 ± 6.1	9222.55 ± 0.57	224 ± 15
7898.11 ± 0.22	151.4 ± 6.3	9266.86 ± 0.60	44.1 ± 4.1
7931.39 ± 0.29	63.1 ± 3.5	9319.02 ± 0.47	253.4 ± 9.8
7971.43 ± 0.33	142.7 ± 5.3	9344.00 ± 0.33	110.7 ± 6.9
8020.56 ± 0.28	86.2 ± 4.5	9362.65 ± 0.37	16.5 ± 6.4
8036.77 ± 0.51	30.3 ± 2.8	9490.33 ± 0.26	159.2 ± 5.5
8099.76 ± 0.26	177.7 ± 5.6	9545.6 ± 1.2	15.0 ± 2.9
8148.00 ± 0.46	39.1 ± 2.9	9559.01 ± 0.98	22.6 ± 3.3
8180.99 ± 0.29	89.2 ± 4.4	9575.31 ± 0.81	26.0 ± 3.3
8328.93 ± 0.35	42.6 ± 2.7	9626.55 ± 0.30	115.2 ± 5.0
8350.40 ± 0.14	6.8 ± 3.2	9707.4 ± 1.9	10.2 ± 2.7
8410.58 ± 0.12*	3.1 ± 1.5	9728.34 ± 0.37	101.6 ± 5.4
8441.8 ± 1.0	12.7 ± 2.3	9802.71 ± 0.87	107.0 ± 9.6
8489.2 ± 2.1	84 ± 15	9816.44 ± 0.48	94.0 ± 8.6
8507.6 ± 1.0	52 ± 13	9863.39 ± 0.74	22.1 ± 2.7
8543.20 ± 0.55	23.4 ± 2.5	9966.2 ± 1.1	28.6 ± 4.3
8589.1 ± 1.0	110.4 ± 7.2	9994.25 ± 0.67	75.9 ± 7.9
8609.42 ± 0.19	26 ± 10	10009.73 ± 0.48	156 ± 11
8642.78 ± 0.19	6.2 ± 2.9	10036.7 ± 1.6	25.6 ± 7.0
8675.04 ± 0.29	80.4 ± 4.1	10044.41 ± 0.68	52.6 ± 7.1
8713.62 ± 0.33	106.1 ± 5.1	10154.42 ± 0.44	96.6 ± 5.2
8765.55 ± 0.42	41.3 ± 3.0	10208.14 ± 0.39	149.8 ± 6.4
8810.90 ± 0.37	65.4 ± 3.9	10356.44 ± 0.43	92.5 ± 4.7
8833.80 ± 0.60	18.0 ± 1.9	10414.95 ± 0.65	77.0 ± 6.4
8863.81 ± 0.84	15.6 ± 2.1	10443.80 ± 0.39	199.4 ± 9.3
8905.6 ± 1.1	9.7 ± 1.6	10475.0 ± 1.3	13.6 ± 2.5
8921.7 ± 1.2	10.7 ± 1.7	10511.4 ± 1.4	9.0 ± 2.2
9000.01 ± 0.30*	84.7 ± 4.4	10580.2 ± 1.3	36.0 ± 6.3

Table 7
Table 3 continued.

E_R (eV)	K (meV)	E_R (eV)	K (meV)
10598.1 ± 1.0	123 ± 16	11967.31 ± 0.51	153.4 ± 8.6
10613.34 ± 0.58	103 ± 12	12030.65 ± 0.91	28.0 ± 2.8
10683.44 ± 0.60	75.1 ± 5.5	12100.51 ± 0.60	106.3 ± 6.2
10704.73 ± 0.10	13.7 ± 6.3	12180.5 ± 1.1	32.1 ± 3.3
10745.98 ± 0.70	92.8 ± 9.6	12280.5 ± 1.1	66.8 ± 6.2
10767.5 ± 1.8	51 ± 17	12323.77 ± 0.65	62.8 ± 5.3
10776.2 ± 1.3	197 ± 28	12444.2 ± 1.0	45.3 ± 4.8
10801.26 ± 0.96	35.3 ± 5.8	12558.99 ± 0.63	101.9 ± 7.0
10851.40 ± 0.41	128.5 ± 7.3	12586.57 ± 0.88	65.2 ± 6.2
10889.87 ± 0.47	152.3 ± 7.6	12664.81 ± 0.41	133.5 ± 7.5
10945.21 ± 0.69	27.7 ± 2.6	12757.70 ± 0.58	153.6 ± 8.8
11085.59 ± 0.84	34.4 ± 3.8	12849.78 ± 0.55	215.8 ± 9.6
11136.20 ± 0.79	69.3 ± 8.6	12908.7 ± 1.1	32.2 ± 3.7
11155.5 ± 1.6	139 ± 49	12979.02 ± 0.96	46 ± 6
11163.3 ± 1.8	150 ± 52	13010.1 ± 1.9	84 ± 18
11211.67 ± 0.47	103.6 ± 6.8	13029.0 ± 1.5	101 ± 18
11240.47 ± 1.06	18.8 ± 2.8	13071.52 ± 0.15	49 ± 18
11317.24 ± 1.95	63.6 ± 8.8	13113.1 ± 1.3	27.0 ± 3.5
11343.58 ± 0.89	54.5 ± 7.4	13233.98 ± 0.55	144.6 ± 7.4
11359.97 ± 0.63	59.8 ± 5.7	13289.15 ± 0.59	74.5 ± 5.8
11409.6 ± 1.0	37.7 ± 4.4	13350.2 ± 1.6	29.3 ± 4.0
11441.92 ± 0.49	91.6 ± 5.6	13384.1 ± 1.3	51.9 ± 6.3
11482.5 ± 1.6	15.5 ± 3.1	13407.4 ± 1.6	50.1 ± 8.0
11525.81 ± 0.14	15.2 ± 6.1	13425.19 ± 0.78	125 ± 11
11542.41 ± 0.46	15.1 ± 6.3	13514.8 ± 1.3	84.1 ± 9.5
11570.32 ± 0.72	70.7 ± 5.8	13551.26 ± 0.54	282 ± 14
11597.56 ± 0.98	36.9 ± 4.0	13654.62 ± 0.76	60.2 ± 5.4
11618.37 ± 0.93	30.2 ± 3.6	13700.12 ± 0.68	103.0 ± 7.0
11675.01 ± 0.68	107.6 ± 8.6	13740.6 ± 1.4	26.9 ± 3.8
11700.45 ± 0.64	116.7 ± 9.1	13767.3 ± 1.5	32.3 ± 4.8
11795.03 ± 0.64	106.6 ± 6.6	13796.7 ± 1.0	49.3 ± 5.2
11821.0 ± 1.4	18.3 ± 3.1	13857.67 ± 0.75	131 ± 10
11856.0 ± 1.6	19.5 ± 3.2	13900.4 ± 1.4	124 ± 12
11883.8 ± 1.5	31.5 ± 5.1	13940.8 ± 1.1	87 ± 10
11911.03 ± 0.45	170.6 ± 9.2	13967.45 ± 0.75	138 ± 11

Data availability

Data will be available in IAEA EXFOR database.

Acknowledgements

This work was supported by the Austrian Science Fund FWF (J3503), the Adolf Messer Foundation (Germany), the UK Science and Technology Facilities Council (ST/M006085/1), and the European Research Council ERC-2015-StG Nr. 677497. We acknowledge also support from MSMT of the Czech Republic.

References

[1] A. Gawlik, et al., Phys. Rev. C 100 (2019) 045804.
[2] D.A. Brown, et al., Nucl. Data Sheets 148 (2018) 1–142.
[3] S. Goriely, Hauser-Feshbach rates for neutron capture reactions (version 8/29/2005), http://www-astro.ulb.ac.be/Html/hfr.html.
[4] A.J. Koning, et al., TALYS-1.9, online at www.talys.eu.
[5] A.J. Koning, et al., Nucl. Data Sheets 113 (2012) 2841, https://tendl.web.psi.ch/tendl_2015/tendl2015.html.
[6] K. Shibata, et al., J. Nucl. Sci. Technol. 48 (2011) 1.
[7] JEFF-3.2, available online: http://www.oecd-nea.org/dbforms/data/eva/evatapes/jeff_32/, 2014.
[8] I. Dillmann, R. Plag, F. Käppeler, T. Rauscher, EFNUDAT Fast Neutrons - scientific workshop on neutron measurements, theory & applications, JRC-IRMM, 2009; online at http://www.kadonis.org.